

renormalized frequencies by their harmonic counterparts and (b) neglecting the unstable modes.

⁷N. Boccara and G. Sarma, *Physics* **1**, 219 (1965).

⁸Unpublished numerical work based on the formalism of Ref. 7 has recently been performed; N. Boccara (private communication).

⁹See N. R. Werthamer [*Phys. Rev. B* **1**, 572 (1970)] for a review of the relevant literature; also, N. R. Werthamer, *Am. J. Phys.* **37**, 763 (1969).

¹⁰A preliminary account of this work has been given in N. S. Gillis and T. R. Koehler, *Bull. Am. Phys. Soc.* **16**, 415 (1971).

¹¹E. W. Kellermann, *Phil. Trans. Roy. Soc. London* **238**, 513 (1940); see also N. S. Gillis, *Phys. Rev. B* **3**, 1482 (1971).

¹²Since the thermal average is with respect to a harmonic density matrix, the thermally averaged potential $\langle V \rangle$ may be evaluated in closed form; see N. S. Gillis, N. R. Werthamer, and T. R. Koehler, *Phys. Rev.* **165**, 951 (1968).

¹³N. S. Gillis, N. R. Werthamer, and T. R. Koehler, *Phys. Rev.* **165**, 951 (1968); N. R. Werthamer, *Phys. Rev. B* **1**, 572 (1970).

¹⁴G. S. Pawley, W. Cochran, R. A. Cowley, and G. Dolling, *Phys. Rev. Letters* **17**, 753 (1966).

¹⁵E. R. Cowley, J. K. Darby, and G. S. Pawley, *J. Phys. C* **2**, 1916 (1969).

¹⁶J. N. Bierly, L. Muldower, and O. Beckman, *Acta Met.* **11**, 447 (1963); E. F. Steigmeier and G. Harbeke,

Solid State Commun. **3**, 1275 (1970).

¹⁷As the longitudinal force constant $\bar{\varphi}_L$ is increased, the frequencies increase also. From Eq. (8) it then follows that $dF_{11}/d\bar{\varphi}_L < 0$ and $d^2F_{11}/d\bar{\varphi}_L^2 > 0$.

¹⁸G. Shirane, R. Nathans, and V. J. Minkiewicz, *Phys. Rev.* **157**, 396 (1967).

¹⁹J. D. Axe, J. Harada, and G. Shirane, *Phys. Rev. B* **1**, 1227 (1970).

²⁰By "close to second order" we mean in the present context that the value of the inverse dielectric susceptibility [or, alternatively, $\omega_{\text{TO}}^2(\Gamma)$] at the transition is much less than its value far from the transition.

²¹The statement that the phonon frequency may not vanish identically in this higher level of approximation is speculative at this point, since the complexity of the fully self-consistent second-order equations (see Ref. 9) precludes a tractable analytical treatment. However, the question of whether the phonon energy vanishes is somewhat academic for real systems, since other complications occur. Indeed, as the phonon energy decreases in magnitude, overdamping may cause the mode of phononlike character to exhibit a purely relaxation-type behavior [see Y. Yamada, G. Shirane, and A. Linz, *Phys. Rev.* **177**, 848 (1969)]. Furthermore, coupling to the strains may also destroy the purely dielectric character of the instability.

²²P. C. Kwok and P. B. Miller, *Phys. Rev.* **151**, 387 (1966).

²³A. F. Devonshire, *Advan. Phys.* **3**, 85 (1954).

Origin of the Linear Term in the Expression for the Approach to Saturation in Ferromagnetic Materials*

Dennis E. Grady[†]

Washington State University, Pullman, Washington 99163

(Received 19 February 1971)

There has been confusion for many years over the origin of the a/H term in the expression for the approach to saturation, $M/M_s = 1 - a/H - b/H^2 + cH$, observed in many ferromagnetic materials. A calculation is presented which suggests that residual internal strain contributes significantly to this term. Internal strain has previously been thought to contribute only to the b/H^2 term. It is further suggested that the a/H term has been overemphasized and has validity only over a limited region of the H axis. The effect of internal strain is deduced from consideration of a problem concerning nonhydrostatic strains induced in slightly porous magnetic material subject to external hydrostatic pressure. A comparison with recent experimental work supports the calculation.

I. INTRODUCTION

There has been continued interest for many years in explaining the various terms which occur in the expression for the approach to saturation observed experimentally in many ferromagnetic materials:

$$\frac{M}{M_s} = 1 - \frac{a}{H} - \frac{b}{H^2} + cH. \quad (1)$$

The cH term has been adequately explained in terms of paraprocesses. The constant in the b/H^2 term has been shown to be

$$b = \frac{8}{105} \frac{K^2}{M_s^2} + \frac{3}{5} \frac{\lambda_s^2 \langle \sigma_i^2 \rangle_{\text{av}}}{M_s^2}, \quad (2)$$

where the first part is due to crystalline anisotropy,¹ and the second part, derived by Becker and Polley,² is considered to be the influence of internal strain on the approach to saturation.

The origin of the a/H term is not well understood. Calculations by Brown³ have shown that dislocation effects can contribute to this term, while Néel⁴ has concluded that stray fields due to nonuniform magnetization may bring about forces

which would contribute to this term. The origin of this term has been investigated experimentally by Parfenov and Voroshilov.⁵ One significant observation noted by these authors was that the constants a and b varied similarly with increasing internal strain in the magnetic material. However, they were unable to substantiate either theory and concluded by still questioning the nature of the a/H term.

The present calculation was motivated by a recent experimental investigation concerning the magnetic properties of slightly porous polycrystalline ferromagnetic materials when subject to external hydrostatic pressure.⁶ The porous material, initially strain-free, experiences nonhydrostatic strain in the vicinity of pores when an external hydrostatic pressure is applied. These nonhydrostatic strain regions, coupled with the magneto-elastic properties of the material, will significantly affect the magnetization curve. In that work (Ref. 6) the magnetization exhibited a strong linear dependence on the variable P/H in the approach to saturation region of the curve. This vividly illustrates the a/H dependence in Eq. (1) and suggests an origin of the constant a .

Specific objectives of the present calculations are the following:

(a) to propose a model for the magneto-elastic behavior of the porous material which predicts the P/H dependence of the magnetization and determines the region of the magnetization curve for which the dependence is valid. Results are compared with the experimental work of Ref. 6;

(b) to suggest that the calculation in (a) is relevant in cases where there is no external applied pressure, but where there are residual internal strains due to internal defects. This would imply that internal strain contributes to the a/h dependence. It was previously thought to contribute only to the b/H^2 dependence. The primary conclusion is that the a/H term is a myth, or has at least been overemphasized. It has approximate validity in a limited range (H neither too large nor too small) of the magnetization curve;

(c) to interpret previous observations (primarily those of Parfenov and Voroshilov) which have not been understood in terms of the conclusion of (b). These interpretations lend further support to the conclusion.

This article is presented in the following order: In Sec. II a model for the magnetic behavior of the porous material subject to external hydrostatic pressure is formulated and a sufficient magnetic energy expression derived. In Sec. III a series solution for the magnetization curve is obtained but is found poorly convergent in the region of interest. A complete numerical solution is presented in Sec. IV. In Sec. V the results of Secs.

III and IV are compared with the experimental work of Ref. 6. In Sec. VI extension of this calculation to the magnetic behavior of material with residual internal strain is suggested and discussed.

II. MODEL FOR POROUS MATERIAL

The first problem, as stated in the Introduction, is to predict the magnetization curve in the approach to saturation region for porous polycrystalline ferromagnetic material subject to external hydrostatic pressure. Porosities contemplated are less than 5%. This is consistent with the work of Ref. 6. Generality is not important here since the ultimate goal is to infer the origin of the a/H term in actual ferromagnetic material from the results of the porosity problem.

The model used to describe the porous material will be developed from the following assumption: The average behavior of an aggregate of randomized and -shaped cavities can be represented by the behavior of a spherical cavity in an infinite isotropic elastic medium. This assumption has been used fruitfully in obtaining the dependence of elastic moduli on porosity in polycrystalline material.^{7,8} An excellent photomicrograph of the situation contemplated is shown on p. 218 of Smit and Wijn.⁹ Illustrated is 5% porous manganese-zinc ferrite.

To obtain the magnetization curve in the region of interest, a magnetic energy expression which adequately describes the material is required. The total energy is usually written¹⁰

$$E = E_H + E_{me} + E_K + E_{ex} + E_d . \quad (3)$$

The first term, $E_H = -\vec{M}_s \cdot \vec{H}$, is the interaction energy with the external applied field. The remaining four terms are, respectively, the magneto-elastic, crystalline anisotropy, exchange, and demagnetizing energies. The magneto-elastic energy will be obtained first. The last three terms are ignored in the present work. Justification is offered later in this section.

To obtain an expression for the magneto-elastic energy, knowledge of the strain distribution about a spherical cavity is required.¹¹ Referring to Fig. 1, the strain field at a distance r from a cavity of radius a , subject to a limiting boundary condition of hydrostatic pressure P and zero traction on the cavity surface, is

$$e_{ij} = -\frac{1}{3}K_T P \delta_{ij} + \frac{P}{4\mu} \frac{a^3}{r^3} \left(3 \frac{x_i x_j}{r^2} - \delta_{ij} \right) . \quad (4)$$

K_T is the compressibility and μ is the shear modulus. It should be mentioned that this approach ignores the magnetostrictive property of the material. The strain error incurred by this approximation is small. Magnetostriction strains are on the order of 10^{-5} . Strains considered in this work

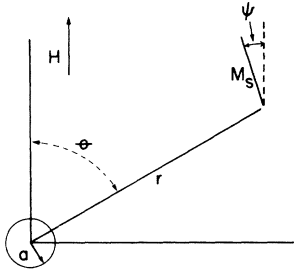


FIG. 1. Spherical cavity of radius a . $M_s \cos \psi$ is the magnetization in the direction of the applied field at the spherical coordinate (r, θ, ϕ) . There is azimuthal symmetry.

are greater than 10^{-3} .

The magneto-elastic energy expression for the isotropic material is obtained by averaging the single-crystal expression

$$E_{me} = b_1(\alpha_1^2 e_{11} + \alpha_2^2 e_{22} + \alpha_3^2 e_{33}) + 2b_2(\alpha_1 \alpha_2 e_{12} + \alpha_2 \alpha_3 e_{23} + \alpha_3 \alpha_1 e_{31}) \quad (5)$$

over random crystal orientation using Eq. (4) for the strain components.¹² This average assumes fixed strains with magnetization in fixed axis. The result is

$$E_{me} = \frac{3}{4} \frac{BP}{\mu} \frac{a^3}{r^3} \cos^2(\psi + \theta), \quad (6)$$

where $B = \frac{2}{5}b_1 + \frac{3}{5}b_2$. The angles are shown in Fig. 1.

Justification for ignoring the remaining energy terms in Eq. (3) is as follows: Consider the crystalline anisotropy energy first. Since the terms in the total energy expression are additive, the contribution of the anisotropy energy to the magnetization in the approach to saturation region may be superimposed. This was done by Parfenov and Voroshilov using the expression

$$\frac{M}{M_s} = 1 - \frac{8}{105} \frac{K^2}{H^2 M_s^2} + \dots \quad (7)$$

derived by Akulov.¹ This will not be done in the present work. Although this refinement would improve the calculation, it tends to obscure the primary objective of the paper.

The exchange energy is commonly expressed in the form

$$E_{ex} A [(\vec{\nabla} \alpha_1)^2 + (\vec{\nabla} \alpha_2)^2 + (\vec{\nabla} \alpha_3)^2],$$

where A is the exchange constant. The exchange energy will be on the order of A/a^2 , where a is the dimension of the spherical cavity. A rough estimate for YIG from molecular field theory is $A \approx 3 \times 10^{-7}$ erg/cm. The cavity dimension is approximately 1μ .^{6,9} This gives an exchange energy on the order of 30 erg/cm³. The magneto-elastic energy for YIG is on the order of $(\frac{3}{4})BP/\mu$. At

$P = 10$ kbar this is 5×10^4 erg/cm³, which is better than three orders of magnitude larger than the exchange energy.

The demagnetizing energy is difficult to assess. The worst imaginable case is a spherical cavity in an otherwise uniform infinite magnetization field. The demagnetizing energy associated with this is

$$E_d = \frac{2}{3} \pi M_s^2 (a^3/r^3) [3 \cos^2 \theta - 1].$$

For YIG this energy is about 10^4 erg/cm³, which is about 20% of the magneto-elastic energy. In practice this is much too high. Such a drastic difference between the exchange and demagnetizing energy would not occur since some form of domain structure would occur in order to reduce this difference.

The justification for ignoring the remaining energy terms is not intended to be rigorous. It does suggest that, in the porous material problem, and in the case of severe internal strain, the magneto-elastic energy is an extremely significant, if not dominant, term. Since this work intends to filter out one term (the magneto-elastic energy) as responsible for the a/H behavior in many magnetic materials, the remaining terms will not be considered.

The surviving energy expression includes the magneto-elastic energy and the interaction energy:

$$E = \frac{3}{4} \frac{BP}{\mu} \frac{a^3}{r^3} \cos^2(\psi + \theta) - H M_s \cos \psi. \quad (8)$$

In magnetic equilibrium the variation of E with respect to the coordinate ψ must be a minimum.

This gives

$$\frac{3}{4} \frac{B}{\mu M_s} \frac{P}{H} \frac{a^3}{r^3} \sin 2(\psi + \theta) - \sin \psi = 0. \quad (9)$$

In order to relate Eq. (9) to the macroscopic magnetization of the porous material, the component of magnetization in the direction of the applied field, $M_s \cos \psi$, must be solved for and integrated over a volume determined by the porosity of the material. This is difficult in practice since Eq. (9), when unfolded in terms of $\cos \psi$, yields a quartic equation. This problem is considered analytically in Sec. III and solved numerically in Sec. IV.

III. ANALYTIC CONSIDERATIONS

Since interest lies in the approach to saturation, a series solution about the point $P/H = 0$, if sufficiently well behaved, would be of value. A solution of this form is possible. Although $\cos \psi$ cannot be solved for explicitly in Eq. (9), implicit derivatives of all orders can be obtained and solved for when evaluated at the point of expansion. The series takes the form

$$\frac{M}{M_s} = \frac{1}{v} \int_v \left(1 + \frac{\partial \cos \psi}{\partial (P/H)} \Big|_0 \frac{P}{H} + \frac{1}{2} \frac{\partial^2 \cos \psi}{\partial (P/H)^2} \Big|_0 \frac{P^2}{H^2} + \dots \right) dV, \quad (10)$$

where the spherical volume of integration is determined by the porosity of the material. When evaluated, the first few terms of the series are

$$\frac{M}{M_s} = 1 - \frac{3}{20} \left(\frac{BP}{\mu M_s H} \right)^2 p + \frac{9}{280} \left(\frac{BP}{\mu M_s H} \right)^3 p + \frac{27}{12320} \left(\frac{BP}{\mu M_s H} \right)^5 p + \dots, \quad (11)$$

where p is the porosity of the material. This series predicts the magnetization curve for the porous material in the approach to saturation region. Explicit dependence on external pressure, applied field, and porosity are shown. It is worth noting that a linear term does not appear.

Comparison of this series with the Becker-Polley expression

$$\frac{M}{M_s} = 1 - \frac{3}{5} \frac{\lambda_s^2 \langle \sigma_i^2 \rangle_{av}}{M_s^2 H^2}, \quad (12)$$

where $\lambda_s = -B/3\mu$ in a magnetically isotropic medium, shows that they are quite similar in a region where the series can be approximated by the first nonvanishing term. This is mentioned for a comparison of the previously predicted effect of internal strain on one hand [see Eq. (2)] and the effect of induced strain in the present problem on the other.

The behavior of this series can best be shown by considering a particular example. With the properties of YIG and a representative value of $P/H=0.1$, which was chosen from values of strain

and applied field used in the work of Ref. 6, the resulting first few terms in the series are

$$M/M_s = 1 - 0.032 + 0.041 + 0.068 + \dots$$

This serves only to illustrate that the functional dependence of M/M_s on P/H in this region is not well represented by the first few terms in the series. In other words, the series does not converge sufficiently fast in this region of the magnetization curve to make its use worthwhile.

It can be shown that the subsequent functional dependence of M/M_s on P/H , following the initial quadratic behavior predicted by Eq. (11), is linear and has a slope given by

$$\frac{dM/M_s}{dP/H} = -\gamma \frac{B}{\mu M_s} p, \quad (13)$$

where γ is a constant independent of material properties. This can be shown analytically, but the calculation represents a last-effort attempt to circumvent the computer. Since a computer solution was ultimately required, this calculation is relegated to the Appendix. This calculation is important, however, since it predicts the linear behavior in a limited region, whereas the numerical solution only strongly suggests it. A glance forward to the numerical solutions in Fig. 2 may help clarify the results of this section.

IV. NUMERICAL SOLUTION

The equilibrium relation (9) was solved for $\cos \psi$ and this term integrated over the required volume by conventional numerical techniques. Solutions for various porosities are shown in Fig. 2. The following observations are noted.

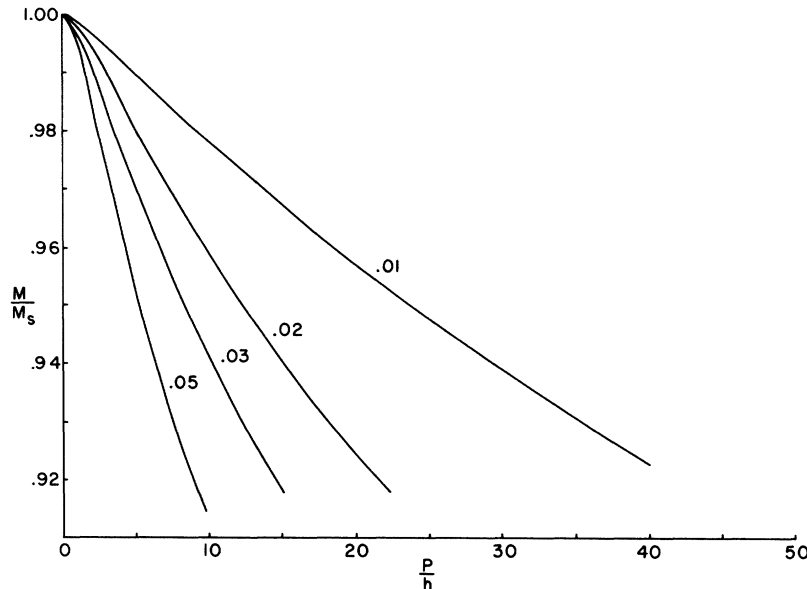


FIG. 2. Numerical solution of pressure-induced deviation from saturation magnetization. $h = H/(\mu M_s/B)$ is the reduced field. Solutions are for porosities of 0.01, 0.02, 0.03, and 0.05. An estimate of the normalized slope, $\gamma = \text{slope}/\text{porosity}$, was approximately $\gamma = 0.21$ for the four curves.

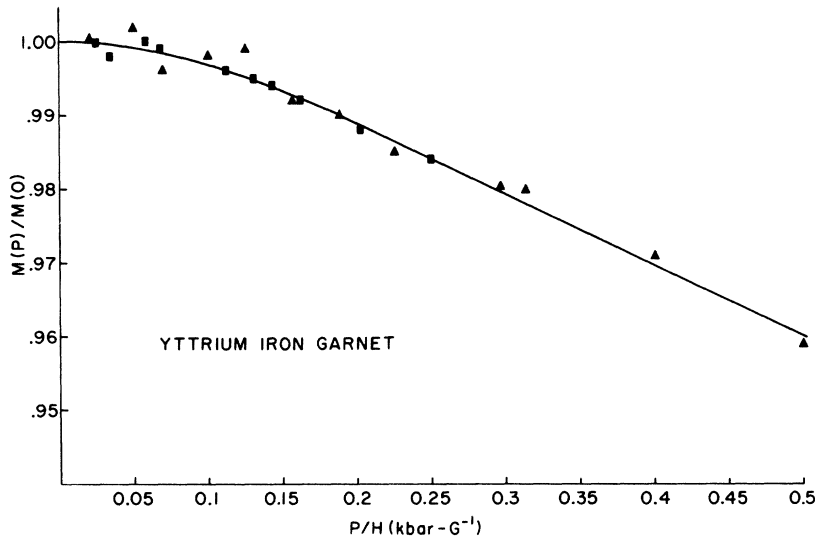


FIG. 3. Magnetization dependence on P/H for 0.02 porosity YIG. The pressure variation is from 0.2 to 4 kbar. \blacktriangle and \blacksquare correspond to 8 and 16 Oe, respectively.

(i) There is initial quadratic behavior in extreme saturation as was expected from the series solution in Eq. (11).

(ii) There is subsequent linear behavior down to almost $\frac{9}{10}$ saturation as expected from Eq. (13).

(iii) The slope in the linear region normalized by the porosity is independent of porosity, in accordance with Eq. (13). A value of $\gamma=0.21$, the constant in Eq. (13), is obtained from each curve in Fig. 2.

(iv) For still lower magnetization the solution deviates from linearity and is asymptotic to $\frac{1}{4}\pi$. This is a consequence of the chosen model but is physically realistic in that this would be the region where cavities would begin to interact and saturation effects would occur.

V. EXPERIMENTAL COMPARISON

Although the work of Wayne *et al.*⁶ suggested this calculation, their data are not well suited for comparison with these theoretical results for the following reasons. First, many of their data are not in the approach to the saturation region. Secondly, they tabulated $M(P)/M(0)$ rather than $M(P)/M_s$ for various values of P and H . The difference, however, is probably due to crystal anisotropy effects which have not been considered in this calculation in order to emphasize the induced strain contribution. Since these are the only data available, this difficulty was ignored and experimental comparison was made which strongly supports the calculation, subject to this limitation. The following comparisons were made:

(i) The data were plotted as a function of P/H . This was found to be a good variable.

(ii) The behavior of YIG was the most carefully considered in Ref. 6. The magnetization curve for YIG was observed to have an initial quadratic

behavior followed by linear behavior as is seen in Fig. 3.

(iii) Slopes in the linear region for the three materials considered (see Figs. 4–6) were obtained and normalized for material properties. The values obtained were $\gamma=0.16$, 0.24, and 0.26, respectively, for YIG, manganese-zinc ferrite, and nickel ferrite. This is to be compared with a value of 0.21 obtained from the numerical solution. This agreement is encouraging since the material properties and porosities of the three ferrites considered are quite varied.

VI. DISCUSSION

A careful analysis of the calculation presented in Secs. II–IV reveals that the linear behavior over a

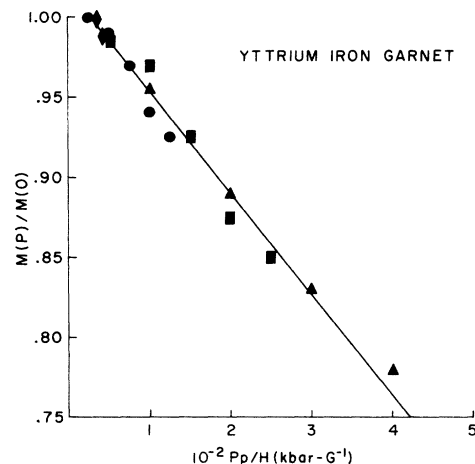


FIG. 4. Magnetization dependence on Pp/H for 0.02 porosity YIG. The pressure variation is from 2 to 20 kbar. \blacktriangle , \blacksquare , \bullet , and \blacklozenge correspond to external applied fields of 8, 16, 39, and 89 Oe, respectively.

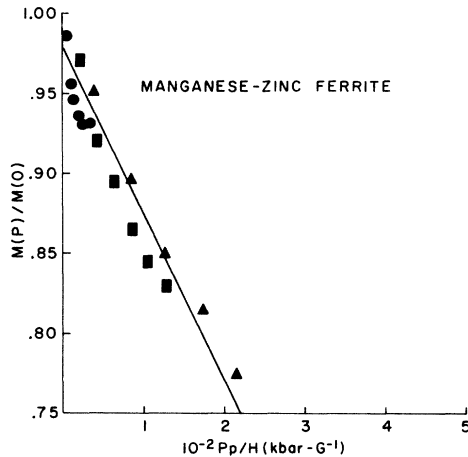


FIG. 5. Magnetization for 0.075 porosity $\text{Mn}_{0.62}\text{Zn}_{0.25}\text{Fe}_{2.13}\text{O}_4$. The pressure variation is from 2 to 12 kbar. \blacktriangle , \blacksquare , and \bullet correspond to external applied fields of 35, 70, and 290 Oe, respectively.

limited region of the $1/H$ axis (see Fig. 2) is a consequence of the $1/r^3$ dependence of the strain field in Eq. (4). This is shown in the Appendix. Since the primary goal is to suggest that this calculation is relevant to magnetic material where there is no external pressure but where there is inherent internal strain, some discussion of the form of this internal strain is necessary. In real material there are many defects around which internal strain will occur. Cavities, inclusions, microcracks, dislocations, impurities, vacancies, interstitial atoms, and grain boundaries will all contribute. Relevance of the present calculation to cases in which internal strain is present assumes that a significant portion of the internal strain falls off as $1/r^3$ from the defect around which it originates. Although the sources of internal strain are not completely understood, several examples may add credibility to this assumption.

(a) A source of internal strain occurs when a material is cooled from some elevated temperature to room temperature. For instance, consider a spherical inclusion of radius a with a thermal expansion coefficient smaller than the surrounding medium. Thermal contraction will create a pressure P_i within this inclusion. The strain field induced in the material surrounding the inclusion is¹¹

$$e_{ij} = -\frac{P_i}{4} \frac{a^3}{r^3} \left(\frac{3x_i x_j}{r^2} - \delta_{ij} \right).$$

Comparison with Eq. (4) reveals a similar $1/r^3$ dependence.

(b) Another source of internal strain occurs from material cold working. Plastic flow is believed to occur in local regions, viz., dislocation slip bands.

This leaves elastic strain locked into the material in other regions. A clear example of this occurs in surface working of cylindrical bars leaving a state of hoop stress in the region below the surface. Approximate this state of stress by a uniform pressure P and again image a spherical inclusion, of compressibility K'_T , in a medium of compressibility K_T and shear modulus μ . The strain field is

$$e_{ij} = -\frac{1}{3} K_T P \delta_{ij} + \frac{1}{3} \frac{K'_T - K_T}{1 + \frac{4}{3} \mu K'_T} p \frac{a^3}{r^3} \left(\frac{3x_i x_j}{r^2} - \delta_{ij} \right).$$

Equation (4) for a spherical pore is a limiting case of this solution. On a smaller scale the strain field about point defects is expected to have a $1/r^3$ dependence. Although the strain field about a line dislocation does not have a $1/r^3$ dependence, the strain field about a dislocation loop does.¹³ In most cases the dominant contributors to internal strain are probably the macroscopic defects such as cavities or inclusions.

This discussion is intended to suggest that in many cases considerable internal strain exhibits a $1/r^3$ dependence about the source defect. If this is true, then results of this calculation qualitatively apply to material containing residual internal strain.

This conclusion serves to explain several observations regarding the approach to saturation which have not been understood.

(i) It has been observed that, in Eq. (1), the quadratic term b/H^2 is dominant for extremely high magnetic fields, while the linear term a/H is dominant in intermediate fields.¹⁴ Figure 2 shows that whether a local internal strain region contri-

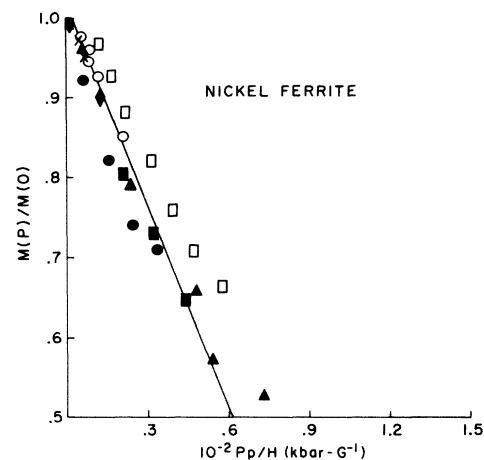


FIG. 6. Magnetization for 0.054 porosity (solid points) and 0.041 porosity (open points) nickel ferrite. The pressure variation is from 2 to 25 kbar. \blacktriangle , \blacksquare , \bullet , \blacklozenge , and \times correspond to external applied fields of 45, 100, 325, 980, and 1960 Oe, respectively. \square and \circ correspond to 100 and 350 Oe, respectively.

butes to quadratic or linear behavior depends on the magnitude of σ_i/H , where σ_i is a measure of internal strain. If H is sufficiently large, this quantity will be small for all σ_i and quadratic behavior observed, while if H is sufficiently small, many local strain regions will contribute to linear behavior and the linear term will dominate.

(ii) Similar variation of a and b with increased internal strain, as observed by Parfenov and Voroshilov, is expected since local strain regions contributing to both linear and quadratic behavior would increase.

(iii) Parfenov and Voroshilov also observed that a is proportional to M_s under temperature variation in nickel. From this calculation, a is proportional to $B/\mu M_s$, as shown by Eq. (13), and since, in nickel, B/μ is proportional to M_s^2 ,¹⁵ this behavior is expected.

VII. CONCLUSION

The primary conclusion is to suggest that the a/H term in the expression for the approach to saturation has been overemphasized. Its origin is in the residual internal strain of magnetic material and it has validity only over a limited region of the H axis. Secondary results are the model and calculation which determine the magnetic behavior of porous magnetic material subject to hydrostatic pressure. It is worth mentioning that this technique suggests a method for controlled investigation of the effects of internal strain on material properties.

ACKNOWLEDGMENT

The author wishes to thank Professor G. E. Duvall for his helpful discussions during the course of this work.

APPENDIX

The following calculation will show that the subsequent functional dependence of M/M_s on P/H , after the initial quadratic behavior, is linear with a slope given by Eq. (13). The magnetic equilibrium relation, Eq. (9), can be written

$$\frac{\gamma^3}{a^3} = \frac{3}{4} \frac{\sin 2(\psi + \theta)}{\sin \Psi} \frac{BP}{\mu M_s H} \quad (14)$$

This, in principle, can be solved for $\cos \psi$, giving

$$\cos \psi = g\left(\frac{u^3}{P/h}, \theta\right),$$

where g is an unknown function, $u = r/a$, and $h = \mu M_s H/B$ is the reduced field. Averaging $\cos \psi$ over a spherical surface gives

$$(\cos \psi)_{\text{av}} = m(u) = k\left(\frac{u^3}{P/h}\right),$$

where k is another unknown function and $m(u)$ is the average normalized magnetization in the direction of the applied field in a spherical shell at a radius r . This can be inverted to obtain

$$u^3 = (P/h)f(m). \quad (15)$$

Again f is unknown. Equation (15) will be used in the following. First an expression for the macroscopic magnetization in the porous material is required. In terms of the proposed model in Sec. II this is

$$\frac{M}{M_s} = \frac{4\pi}{3} \frac{1}{\pi \gamma_0^3} \int_a^{\tau_0} m r^2 dr$$

or

$$\frac{M}{M_s} = 3p \int_1^{\tau_0/a} m u^2 du,$$

where $p = a^3/\gamma_0^3$ is porosity.

In anticipation of linear behavior consider

$$\frac{dM/M_s}{dP/h} = 3p \int_1^{\tau_0/a} \left. \frac{\partial m}{\partial P/h} \right|_u u^2 du.$$

The mathematical identity

$$\left. \frac{\partial m}{\partial P/h} \right|_u = - \left. \frac{\partial u}{\partial P/h} \right|_m \left. \frac{\partial m}{\partial u} \right|_{P/h}$$

with Eq. (15) gives

$$\left. \frac{\partial m}{\partial P/h} \right|_u = - \frac{f(m)}{3u^2} \left. \frac{\partial m}{\partial u} \right|_{P/h},$$

and therefore

$$\frac{dM/M_s}{dP/h} = -p \int_1^{\tau_0/a} f(m) \left. \frac{\partial m}{\partial u} \right|_{P/h} du.$$

In a region where the magneto-elastic energy dominates at the lower integration limit while the magnetic energy dominates at the upper limit, the integral transforms to

$$\frac{dM/M_s}{dP/h} = -p \int_{\tau/4}^1 f(m) dm. \quad (16)$$

This shows the anticipated linear behavior which is expected to occur in some region of the P/h axis. Equation (16) is Eq. (13) with γ given by the integral expression.

*Research sponsored by the U. S. Air Force Office of Scientific Research under Contract No. AFOSR-69-1758.

†Present address: Stanford Research Institute, Menlo Park, Calif. 94025.

¹N. S. Akulov, Z. Physik **69**, 882 (1931).

²R. Becker and H. Polley, Ann. Physik **37**, 534 (1940).

³W. E. Brown, Phys. Rev. **58**, 736 (1940); **60**, 132 (1941).

- ⁴L. Néel, *J. Phys. Radium* **5**, 184 (1948).
⁵V. V. Parfenov and V. P. Voroshilov, *Phys. Metals Metallog. (USSR)* **13**, 340 (1962); **13**, 502 (1962).
⁶R. C. Wayne, G. A. Samara, and R. A. LeFever, *J. Appl. Phys.* **41**, 633 (1970).
⁷A. Buch and S. Goldschmidt, *Materials Sci. Eng.* **5**, 111 (1970).
⁸J. K. Mackenzie, *Proc. Phys. Soc. (London)* **62**, 2 (1950).
⁹J. Smit and H. P. J. Wijn, *Ferrites* (Wiley, New York, 1959), p. 119.
¹⁰C. Kittel, *Rev. Mod. Phys.* **21**, 541 (1949).
¹¹This and later results are limiting cases of a general solution attributed to Lamé. See also L. O. Landau and E. M. Lifshitz, *Theory of Elasticity* (Addison-Wesley, Reading, Mass., 1955), p. 20.
¹²See, for instance, R. R. Birss, *Proc. Phys. Soc. (London)* **75**, 8 (1960).
¹³J. P. Hirth and J. Lothe, *Theory of Dislocations* (McGraw-Hill, New York, 1968).
¹⁴A. H. Morrish, *The Physical Principles of Magnetism* (Wiley, New York, 1965), p. 395.
¹⁵E. W. Lee, *Rept. Progr. Phys.* **28**, 184 (1955).

Some Critical Properties of the Eight-Vertex Model*

Leo P. Kadanoff and Franz J. Wegner[†]

Department of Physics, Brown University, Providence, Rhode Island 02912

(Received 16 July 1971)

The eight-vertex model solved by Baxter is shown to be equivalent to two Ising models with nearest-neighbor coupling interacting with one another via a four-spin coupling term. The critical properties of the model in the weak-coupling limit are in agreement with the scaling hypothesis. In this limit where $\alpha \rightarrow 0$, the critical indices obey $\gamma/\gamma_0 = \beta/\beta_0 = \nu/\nu_0 = 1 - \frac{1}{2}\alpha$, $\delta/\delta_0 = \eta/\eta_0 = 1$, with the subscripts zero denoting the index values for the ordinary two-dimensional Ising model.

In a recent publication, Baxter¹ has found the free energy for the eight-vertex problem and shown that α is a continuous function of the interaction constants. This continuous variation of a critical index contradicts the hypothesis of smoothness² or universality³ often postulated for near-critical problems.

One way of seeing the source of this behavior is to rephrase the eight-vertex problem as an Ising model.⁴ Imagine a spin placed at the interstitial points of the lattice as in Fig. 1. An arrow to the right (or upward) corresponds to the case in which the adjacent spins are parallel; a leftward or downward arrow makes the adjacent spins antiparallel. Then, the four combinatorial factors a , b , c , and d corresponding to the vertices shown can all be represented by a factor in the partition function

$$Ae^{K^-\sigma_1\sigma_4 + K^+\sigma_2\sigma_3 + \lambda\sigma_1\sigma_2\sigma_3\sigma_4},$$

and we obtain the complete partition function

$$\sum_{\{\sigma_r = \pm 1\}} \prod_{j,k} A \exp(K^+\sigma_{j,k}\sigma_{j+1,k+1} + K^-\sigma_{j+1,k}\sigma_{j,k+1} + \lambda\sigma_{j,k}\sigma_{j+1,k+1}\sigma_{j+1,k}\sigma_{j,k+1}), \quad (1)$$

in which next-nearest-neighbor spins are coupled by interaction constants K^\pm depending upon the direction of the diagonal. The factor λ couples all four spins. The precise connection is that

$$a = Ae^{K^+ + K^- + \lambda}, \\ b = Ae^{-(K^+ + K^-) + \lambda},$$

$$c = Ae^{K^+ - K^- - \lambda}, \\ d = Ae^{-(K^+ - K^-) - \lambda}. \quad (2)$$

The constant A does not, of course, enter into the critical properties.

The Baxter solution shows that this Ising-type problem has a very new kind of singularity at the critical point, namely, one in which the singularity in the specific heat as $\epsilon \sim (b + c + d - a)/a$ goes to zero is of the form $\epsilon^{-\alpha}$ with α being a function of the parameters, namely,⁵

$$\sin \frac{\pi\alpha}{4(1 - \frac{1}{2}\alpha)} = \tanh 2\lambda. \quad (3)$$

This result seems at first to contradict the smoothness hypothesis² which suggests that critical indices should not change their value unless there is a symmetry change. However, this eight-vertex model certainly has a different set of symmetries than the usual two-dimensional Ising model. Notice that at $\lambda = 0$, the lattice with $j + k =$ (even integer) does not interact with the lattice with $j + k =$ (odd integer). Even at $\lambda \neq 0$ for $T > T_c$, i. e., $\epsilon > 0$, the spins on these two sublattices are uncorrelated. Therefore, the Ising form of the eight-vertex model can be viewed as having two lattices with "independent" ferromagnetic transitions which occur at exactly the same temperature. The coupling between these two lattices is of the form

$$\lambda \sum_r u_r; \quad u_r = \mathcal{G}_r^{(1)} \mathcal{G}_r^{(2)}, \quad (4)$$